Evidence for El Niño–Southern Oscillation (ENSO) influence on Arctic CO interannual variability through biomass burning emissions

S. A. Monks,[1] S. R. Arnold,[1] and M. P. Chipperfield[1]

[1]   A global chemical transport model is used in conjunction with measurements from surface stations to study the importance of biomass burning and meteorology in driving Arctic carbon monoxide (CO) interannual variability (IAV). Simulations with yearly varying fire emissions capture 66%–93% of CO IAV and a simulation with yearly varying meteorology but fixed fire emissions captures 0–25%, showing that biomass burning variability is the dominant driver of surface CO IAV. Observed CO anomalies are found to be significantly correlated with El Niño ($0.58 < r < 0.64$, 99% confidence level (CL)) and results indicate that this is due to ENSO's influence on fire emissions. Boreal Alaska, Canada and north-east Siberia are found to contribute 59% to total Arctic fire CO and 67% to Arctic fire CO IAV. Analysis of meteorological fire drivers in these regions suggests that ENSO affects winter/spring precipitation, driving the Arctic/ENSO relationship. **Citation:** Monks, S. A., S. R. Arnold, and M. P. Chipperfield (2012), Evidence for El Niño–Southern Oscillation (ENSO) influence on Arctic CO interannual variability through biomass burning emissions, *Geophys. Res. Lett.*, *39*, L14804, doi:10.1029/2012GL052512.

1.   Introduction

[2]   The Arctic was long believed to be clean and unpolluted; however, by the mid-1980s it was well understood that high concentrations of pollutants observed in this remote region during winter and spring were a consequence of long-range transport of anthropogenic emissions from Eurasia and North America [*Rahn*, 1985]. Chemical traces found in ice cores [*Legrand et al.*, 1992] and plumes observed during flights [e.g., *Wofsy et al.*, 1992] and at surface stations [*Stohl et al.*, 2007] show increasing evidence that biomass burning emissions are also transported to the Arctic in spring and summer. Forest fires emit large quantities of ozone precursors (CO, NO_x, non-methane hydrocarbons) and aerosols to the atmosphere, and therefore have the potential to affect the radiative budget [*Randerson et al.*, 2006]. Arctic atmospheric composition in the summer and autumn has received less attention compared to winter and spring due to more effective pollutant removal mechanisms and less efficient poleward transport from the mid-latitudes. However, summer may be particularly important in terms of local radiative forcing [*Shindell*, 2007]. The boreal forests of Canada, North America and Siberia have peak fire emissions during summer [*van de Werf et al.*, 2010] and are ideally located to affect Arctic trace gas and aerosol burdens and therefore climate.

[3]   Weather and climate factors, such as temperature, precipitation and relative humidity, are important in controlling fire activity by influencing fuel moisture, with more severe fires (with larger area burned) occurring under drier conditions in the boreal regions [e.g., *Fauria and Johnson*, 2008; *Bartsch et al.*, 2009]. Biomass burning exhibits a high interannual variability (IAV) [*van de Werf et al.*, 2006] with many studies showing a relationship between regional fire activity and climate indices [e.g., *Westerling et al.*, 2006]. Specifically, boreal fires have been linked to the El Niño - Southern Oscillation (ENSO), North Atlantic Oscillation (NAO), Arctic Oscillation (AO), Pacific Decadal Oscillation (PDO) and the Atlantic Multi-decadal Oscillation (AMO) [e.g., *Balzter et al.*, 2007; *Skinner et al.*, 2006; *Le Goff et al.*, 2007; *Beverly et al.*, 2011]. In addition to this, modelling studies have shown that due to increased temperatures and drying in the boreal forests, fire risk may increase in the future [e.g., *Flannigan et al.*, 2009; *Liu et al.*, 2010] with potential consequences for the Arctic.

[4]   As Arctic burdens of pollutants are predominately from non-local sources, changes in meteorology and natural climate variability, which determine the transport efficiency of emissions to the Arctic, are also important. The NAO is a major mode of atmospheric variability in the Northern Hemisphere and has been found to affect the Arctic CO burden through enhanced poleward transport during positive NAO phases [*Eckhardt et al.*, 2003]. It has also been suggested that during cold phases of ENSO, poleward transport may be hindered, causing an anomalously low CO column over Alaska [*Fisher et al.*, 2010]. Climate change may affect large-scale circulation patterns, natural climate variability and the temperature gradient between the Arctic and lower latitudes, possibly resulting in enhanced pollutant transport to the Arctic, giving a need to better understand how meteorological variability influences the Arctic [*Shindell et al.*, 2008].

[5]   Here we use modelled CO as a tracer to investigate how variability in meteorology and biomass burning emissions contribute to observed Arctic CO IAV. We also explore possible links between natural climate variability and Arctic CO IAV, and the mechanisms that may drive them.

2.   Model and Data Description

2.1.   TOMCAT Model Description and Set-up

[6]   TOMCAT is a three-dimensional (3-D) Eulerian global chemical transport model (CTM) which has been previously

[1]Institute for Climate and Atmospheric Science, School of Earth and Environment, University of Leeds, Leeds, UK.

Corresponding author: S. A. Monks, Institute for Climate and Atmospheric Science, School of Earth and Environment, University of Leeds, Leeds LS2 9JT, UK. (s.a.monks@leeds.ac.uk)

Table 1. Multi-station Multi-annual Mean Percent Contributions to Absolute Arctic Fire CO and Arctic Fire CO IAV From Different Emission Regions, Averaged Over the 5 Surface Stations Shown in Figure 1 and 1997–2009[a]

Region	CO Contribution (%)	IAV Contribution[b] (%)	r[c]
NESI (45–80 N, 115–179 E)	33.8	44.1	0.38
ALCA (45–47 N, 190–308 E)	24.6	23.3	**0.62**
NCSI (45–80 N, 50–115 E)	10.3	9.8	0.18
NHAF (0–35 N, 342.5–50 E)	7.3	1.3	−0.04
EQAS (10 N–12 S, 90–150 E)	7.0	12.8	**0.68**
SEAS (10–45 N, 90–150 E)	4.4	3.4	**0.55**
SHAF (0–35 S, 342.5–60 E)	4.1	0.5	**0.66**
EURO (35–70 N, 342.5–50 E)	2.8	1.3	−0.21
AUST (12–40 S, 110–160 E)	2.5	0.3	−0.36
NSAM (12 N–20 S, 280–325 E	2.1	1.3	**0.63**
WNAM (22–45 N, 230–265 E)	0.7	0.5	−0.28
CEAM (8–22 N, 250–280 E)	0.7	0.8	**0.64**
ENAM (22–45 N, 265–300 E)	0.6	0.4	0.44
CSAS (5–45 N, 50–90 E)	0.6	0.2	−0.36
SSAM (20–55 S, 280–325 E)	0.2	0.1	−0.02

[a]NESI = north-eastern Siberia, ALCA = Alaska and Canada, NCSI = central Siberia, NHAF = N.H. Africa, EQAS = equatorial Asia, SEAS = Southern Asia, SHAF = S.H. Africa, EURO = Europe, AUST = Australia, NSAM = N.H. South America, WNAM = western North America, CEAM = Central America, ENAM = eastern North America, CSAS = central-southern Asia, SSAM = S.H. South America. Correlation coefficients have been calculated between the El Niño 3.4 index and the total fire CO emitted during the defined burn season in each region over the 1997–2009 period.

[b]Calculated from $IAV_{ij} = \frac{\sigma_{ij}}{\sum \sigma_{ij}} \times 100$, where IAV_{ij} is the percent contribution to IAV of tracer i, at station j, and σ_{ij} is the standard deviation.

[c]Correlations shown in bold are significant at the 95% confidence level.

used for tropospheric chemistry studies [e.g., *Arnold et al.*, 2005; *Sodemann et al.*, 2011]. The model is forced using meteorological data from the European Centre for Medium-Range Weather Forecasts (ECMWF) ERA-Interim analyses. Descriptions of tracer advection, sub-scale treatment of boundary layer mixing and moist convection are given by *Chipperfield* [2006]. For these simulations the model has 31 levels, which extend from the surface to 10 hPa, and a horizontal resolution of $2.8° \times 2.8°$.

[7] Four simulations were performed for 1997–2009. The first (vbb_vmet) used yearly varying biomass burning emissions and meteorology and the second (cbb_vmet) used climatological biomass burning emissions (averaged over 1997–2009) and yearly varying meteorology. Two additional simulations used yearly varying biomass burning emissions but repeated meteorology from May 1997 to April 1998 (vbb_met97) and January to December 2001 (vbb_met01), respectively. The El Niño index remained positive for May 1997–April 1998 and both the NAO and El Niño indices were neither strongly positive nor negative in 2001, providing two contrasting cases of meteorology.

[8] For these experiments, CO tracers were decayed by 3-D global OH fields from *Patra et al.*, [2011], which varied monthly but contained no interannual variability. CO emissions were taken from the IPCC AR5 anthropogenic estimates for the year 2000 [*Lamarque et al.*, 2010], the POET natural emissions database [*Olivier et al.*, 2003] and the GFED v3.1 biomass burning dataset covering 1997–2009 [*van de Werf et al.*, 2010]. GFED v3.1 CO fire emissions are estimated from satellite-derived area burned data and fuel loads calculated from a biogeochemical model. Secondary

production of CO from hydrocarbons was accounted for by increasing all of the direct anthropogenic and biomass burning CO emissions by 18.5% and 11%,respectively following the estimates of *Duncan et al.*, [2007]. Production of CO from biogenic isoprene was accounted for by scaling isoprene emissions from 568 Tg(C_5H_8)/year to yield 127 Tg(CO)/year, assuming isoprene to be oxidised immediately to CO, following the treatment of *Duncan et al.*, [2007]. Secondary production of CO from CH_4 was calculated online by decaying a monthly mean TOMCAT CH_4 field by OH and assuming that each oxidised molecule of CH_4 produces one molecule of CO. In addition to the main CO tracer, additional tracers were included in the vbb_vmet simulation to quantify the contribution to Arctic CO from fire emissions in 15 different regions (see Table 1 for longitude/latitude boundaries).

2.2. Data Description

[9] CO anomalies were calculated from monthly mean surface observations taken from the World Data Centre for Greenhouse Gases (WDCGG) (http://gaw.kishou.go.jp/wdcgg/). The monthly means were calculated from flask samples that were analysed for CO using gas chromatography [*Novelli et al.*, 1998].

[10] Correlations between ENSO and the meteorological drivers of fires were calculated using the El Niño 3.4 index and ECMWF ERA-Interim data. The El Niño 3.4 index was taken from the NOAA Climate Prediction Centre (www.cpc.ncep.noaa.gov/data/indices/nino34.mth.ascii.txt) and is used to define the different phases of ENSO. The index is the anomaly relative to the 1950–2000 average sea-surface temperature (SST) in the region 5°N–5°S, 120°–170°W and captures the coupled impacts of El Niño and the Southern Oscillation [*Trenberth*, 1997]. To analyse the meteorological drivers of fires, monthly mean precipitation, relative humidity and temperature were taken from the ECMWF ERA-Interim analyses at a horizontal resolution of $2.5° \times 2.5°$.

3. Results

3.1. Importance of Meteorology and Fire Emissions for Arctic IAV

[11] Figure 1 shows annual mean CO anomalies calculated for each of the four model simulations and observations along with the coefficients of determination (r^2), which give a measure of how much each model simulation captures the observed interannual variability. The vbb_vmet simulation, which is most realistic due to the use of yearly varying meteorology and fire emissions, captures most of the observed CO anomaly at 4 out of the 5 stations ($r^2 > 0.85$, root-mean-square error (RMSE) = 3.7–5.6 ppbv), giving confidence in the model's ability to capture Arctic CO IAV. This simulation also shows that variability in meteorology and fire emissions together account for 66%–91% of observed CO IAV at the surface. Considering variability in meteorology alone in cbb_vmet (with the use of climatological fire emissions) the model only captures 0–25% of CO IAV. For this simulation, ICE and ALT exhibit the highest values of r^2, suggesting that these stations are more sensitive to yearly changing circulation patterns compared to BRW and ZEP. Furthermore, there is very little difference between the three model experiments, vbb_vmet, vbb_met01 and vbb_met97, which are forced by different meteorology,
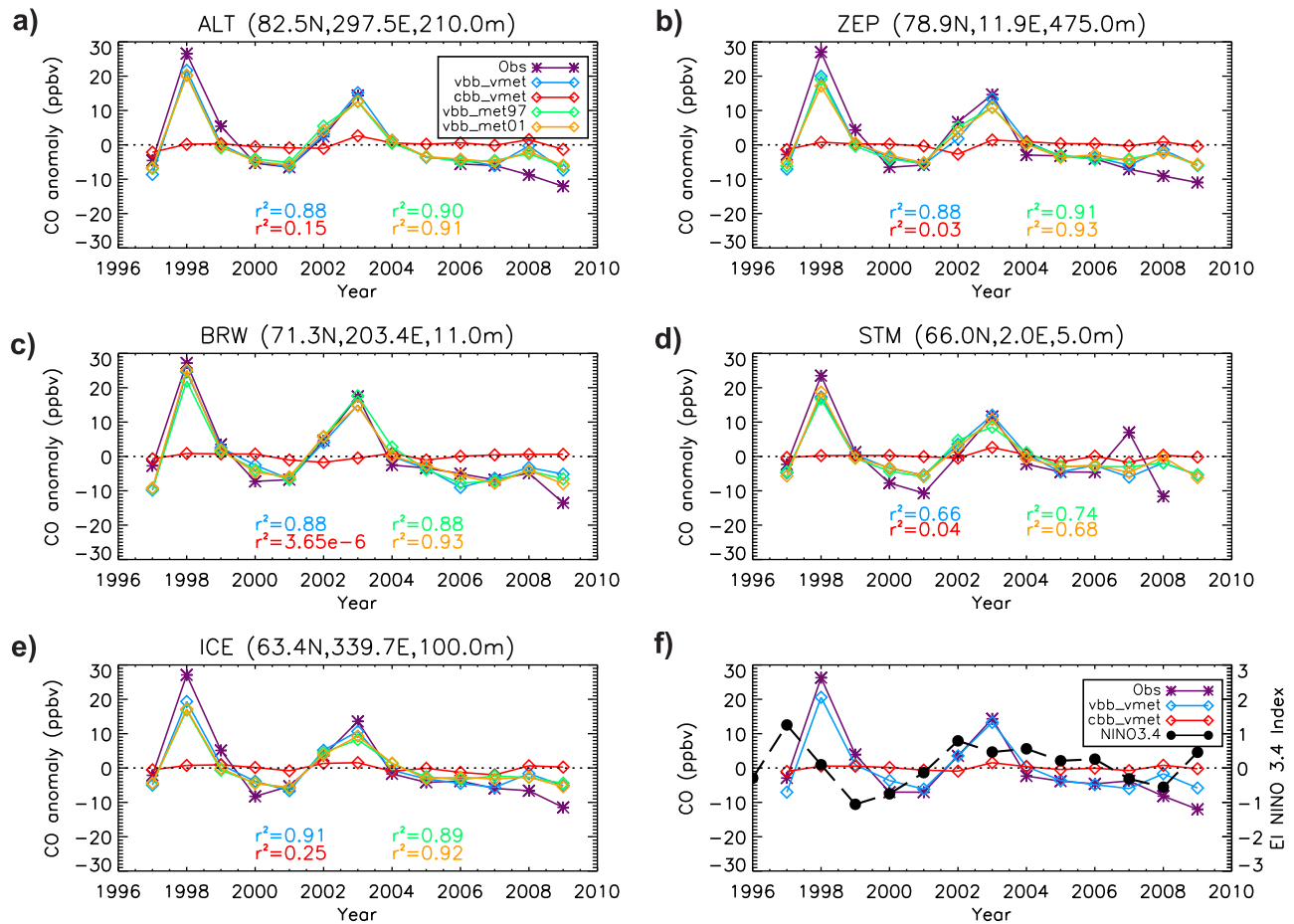
Figure 1. Annual mean observed and modelled CO anomalies (ppbv) relative to the 1997–2009 mean. (a–e) Anomalies at five surface stations (locations shown in Figure S1) (model anomalies shown for vbb_vmet, vbb_met97, vbb_met01 and cbb_vmet simulations). (f) multi-station mean observed and simulated CO anomalies compared to the annual mean El Niño 3.4 index. (N.B. Observed CO has missing data at Alert between 01/10/2004–28/02/2005). Absolute comparisons of CO from vbb_vmet to observations are shown in Figure S2 (r = 0.72–0.92, RMSE = 16.9–24.8 ppbv, which is at the lower end of the 17–40 ppbv range of RMSEs found in the Arctic model intercomparison study by *Shindell et al.* [2008]).

affirming that meteorology has a smaller impact on Arctic surface CO IAV compared to fire emission variability during 1997–2009. A previous global study by *Szopa et al.* [2007] found ICE and STM to be more influenced by meteorology compared to BRW. However, they concluded that CO IAV between 1997–2001 at the Arctic surface was almost equally driven by meteorology and fire emissions, which differs to the conclusions drawn here. The correlations shown in Figure 1 show better overall agreement with the observed CO anomalies than those calculated by *Szopa et al.* [2007] and could be explained by model differences in fire emissions and meteorological data.

[12] Multi-station, multi-year mean percent regional contributions to total fire CO and fire CO IAV in the Arctic have been calculated from the regional fire CO tracers (see Table 1). Fire emissions in the boreal regions of north-east Siberia (NESI) and Alaska and Canada (ALCA) are the largest contributors to Arctic fire-sourced CO (34% and 25%, respectively) and Arctic fire CO IAV (44% and 23%, respectively), showing Arctic fire CO IAV to be largely controlled by fire emissions in these boreal regions. These two regions also contribute the largest fraction to Arctic fire CO

in summer and autumn (see Figure S3 in the auxiliary material), which is also when fires have the largest percent contribution to total Arctic CO (13–24%).[1] This seasonality may have important implications for climate, as local Arctic radiative forcing is believed to be dominant during summer [*Shindell*, 2007]. The third largest source of Arctic fire CO (10%) is from central Siberia (NCSI),which is also the fourth largest contributor to Arctic fire CO IAV (10%). However, in comparison to ALCA and NESI, its contribution to fire IAV is much smaller. Equatorial Asia (EQAS) is the third most important contributor to IAV (13%) but it only contributes 7% to total fire CO.

3.2. Links Between Arctic CO IAV and Climate Oscillations

[13] As we have shown boreal fire emissions to be the dominant source of Arctic CO IAV, we now consider possible links between natural climate variability and Arctic CO IAV in these regions. Lag-correlations were calculated

---

[1]Auxiliary materials are available in the HTML. doi:10.1029/2012GL052512.
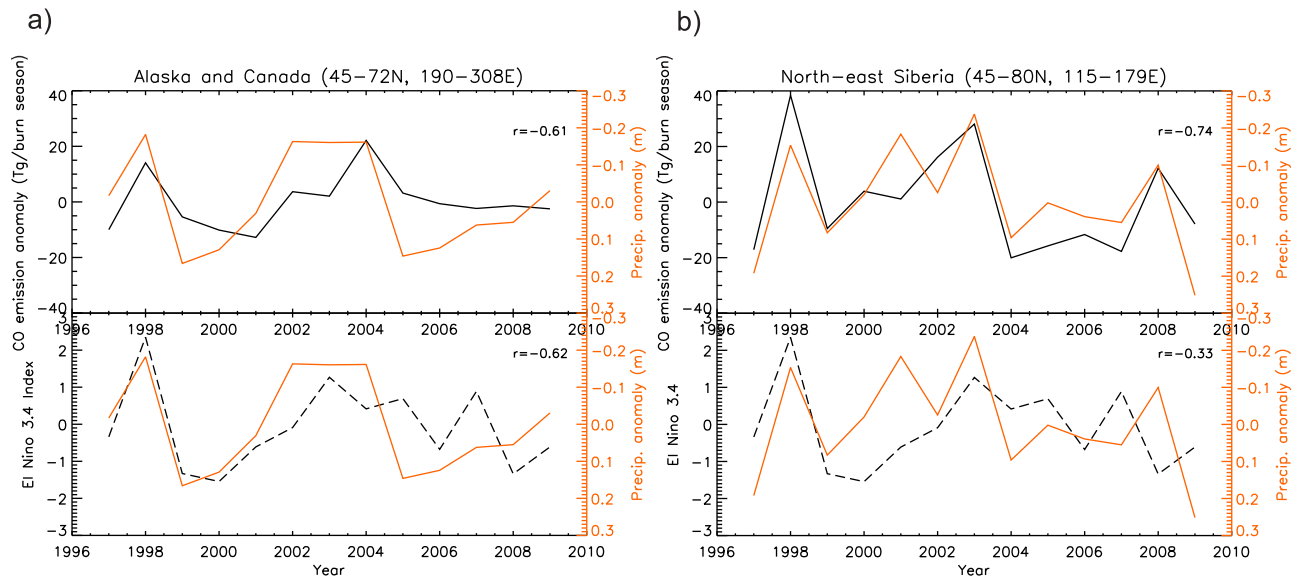
Figure 2. Total precipitation anomalies prior to the burn season (orange) between 1997–2009 over (a) the Alaska and Canada region and (b) the north-east Siberia region along with (top) the annual mean forest fire emissions anomaly and (bottom) the El Niño 3.4 Index (averaged over November to February). Pearson's correlation coefficients between the two time series are shown in the top right corners of each panel (r-values > 0.55 are significant at 95% CL).

between the monthly mean observed and simulated CO anomalies at the Arctic surface stations and several climate oscillation indices (see Figures S4–S8). No significant correlations were found between modelled or observed anomalies and the AO, NAO and Pacific North American (PNA) indices, suggesting that climate variability associated with these oscillations did not play a significant role in Arctic surface CO IAV during 1997–2009. Lag correlations between the monthly El Niño 3.4 index and the monthly observed CO anomalies yield significant correlations (0.58 < r < 0.64, 99% confidence level (CL)), which are at a maximum with a lag of 10 or 11 months (see Figure S7). This relationship is only reproduced in the model when yearly varying emissions are used (0.47 < r < 0.56, 99% CL). This correlation indicates that ENSO may be influencing fire emissions in regions where fire emissions are transported to the Arctic. The lag is likely to be mostly due to the time between the maximum ENSO phase (usually between November and February) and the onset of the fire season in the regions that are important sources of Arctic fire CO. Figure 1f shows the multi-station annual mean CO anomalies, from observations and the vbb_vmet and cbb_vmet simulations, along with the El Niño 3.4 index. Similarities between the patterns of the index and the observed and modelled vbb_vmet CO anomalies are evident but have an offset of 1 year (due to the lag). The PDO index yields a similar lag-correlation pattern as found with the El Niño index but with lower correlations (0.43 < r < 0.48, 99% CL, see Figure S8). This is likely to be due to the PDO and El Niño 3.4 indices being closely linked (annual mean r = 0.82). The El Niño 3.4 index represents shorter-term SST variability in the equatorial Pacific compared to the PDO, which is likely to be more important for fire variability on the time-scales considered here (13 years), therefore explaining why the El Niño index yields the highest correlation. It is worth noting that the multi-decadal cycle of the

AMO may be important for longer-term Arctic variability as it has been shown to be linked to long-term variability in boreal fires but may also play a role in affecting the ENSO/Arctic CO relationship as the AMO phase is also believed to change the strength of the ENSO's influence on fires [*Kitzberger et al.*, 2007]. This has not been considered here due to the relatively short period of time being considered.

3.3. Influence of ENSO on Fire Emissions in the Boreal Regions

[14] Table 1 also shows the correlations calculated between the El Niño index and the total fire CO emissions during the burn season (the burn season was defined for each region as the 5–6 month period with the maximum CO fire emissions). The top two contributors to fire CO and fire CO IAV, NESI and ALCA, have r-values of 0.38 and 0.62, respectively. indicating that during warm phases of ENSO (El Niño years) these two regions may experience greater fire emissions. As these two regions dominate the IAV of Arctic CO (see Table 1), ENSO's influence on fire emissions in these regions may explain the significant correlation found between observations at the Arctic surface stations and El Niño. Other positive correlations were also found between regional fire emissions and El Niño, for example in EQAS (r = 0.68), which also contributed 13% to Arctic fire IAV.

[15] ENSO is known to have worldwide impacts on temperature and precipitation [*Ropelewski and Halpert*, 1986] and, as already mentioned, has been shown to be related to fire activity in different regions. To investigate the correlation between El Niño and Arctic CO further, the relationships between fire emissions and temperature, relative humidity and precipitation, were considered in the boreal regions of Alaska, Canada and Siberia. Correlations were calculated for both the burn season emissions and the El Niño index with precipitation, relative humidity and

temperature, both before the burn season (November to April) and during the burn season (May to August). Total precipitation prior to the burn season (during winter and spring) was found to be significantly negatively correlated with CO emissions (see Figure 2) in both Alaska and Canada (r = −0.61) and north-eastern Siberia (r = −0.74), indicating that reduced rainfall in the winter and spring is associated with greater fire emissions. Wintertime precipitation is important for snowfall accumulation and these correlations are in agreement with studies that have shown anomalously low snow cover to be associated with a higher fire risk [e.g., *Westerling et al.*, 2006]. In addition to this, models have shown precipitation to be an important driver of area burned interannual variability in the boreal forests [e.g., *Crevoisier et al.*, 2007].

[16] Precipitation prior to the burn season in Alaska and Canada was found to be significantly negatively correlated with the El Niño index (r = −0.62), indicating that ENSO could be modulating fire emissions in this region through its influence on precipitation. Other studies have also linked anomalously large boreal fires during dry conditions in North America/Canada to natural climate variability associated with El Niño events, supporting the correlations calculated here [e.g., *Fauria and Johnson*, 2008]. In north-eastern Siberia the El Niño index is also negatively correlated with precipitation (r = −0.33) but is not significant at the 95% confidence level. In eastern Siberia some studies have shown the fire regime to be linked to both the Arctic Oscillation (AO) and El Niño [e.g., *Balzter et al.*, 2007], possibly explaining why the present study does not yield a significant correlation with the El Niño 3.4 index alone.

4. Discussion

[17] Our results clearly show that biomass burning is the dominant driver of surface Arctic CO IAV. Emissions from boreal fires were shown to be the largest source of Arctic fire CO and variability, with the largest CO contributions during summer and autumn. Studies have shown that increased temperatures and drying in the boreal forests are likely to increase the intensity and frequency of future fires in this region [e.g., *Flannigan et al.*, 2009], and as fire emissions contain ozone precursors and aerosol, this may have implications for Arctic climate. This work is the first to show that a relationship may exist between ENSO and Arctic CO IAV through ENSO's influence on fires and suggests that future climate variability may play an important role in determining the future burdens of pollutants in this climate sensitive region.

[19] The Editor thanks the two anonymous reviewers for assisting in the evaluation of this paper.

References

Arnold, S. R., M. P. Chipperfield, and M. A. Blitz (2005), A three-dimensional model study of the effect of new temperature-dependent quantum yields for acetone photolysis, *J. Geophys. Res.*, 110, D22305, doi:10.1029/2005JD005998.
Balzter, H., F. Gerard, C. George, G. Weedon, W. Grey, B. Combal, E. Bartholome, S. Bartalev, and S. Los (2007), Coupling of vegetation growing season anomalies and fire activity with hemispheric and regional-scale climate patterns in central and east Siberia, *J. Clim.*, 20, 3713–3729.
Bartsch, A., H. Balzter, and C. George (2009), The influence of regional surface soil moisture anomalies on forest fires in Siberia observed from satellites, *Environ. Res. Lett.*, 4, 045021, doi:10.1088/1748-9326/4/4/045021.
Beverly, J. L., M. D. Flannigan, B. J. Stocks, and P. Bothwell (2011), The association between Northern Hemisphere climate patterns and interannual variability in Canadian wildfire activity, *Can. J. Forest Res.*, 41, 2193–2201, doi:10.1139/x11-131.
Chipperfield, M. P. (2006), New version of the TOMCAT/SLIMCAT offline chemical transport model: Intercomparison of stratospheric tracer experiments, *Q. J. R. Meteorol. Soc.*, 132, 1179–1203.
Crevoisier, C., E. Shevliakova, M. Gloor, C. Wirth, and S. Pacala (2007), Drivers of fire in the boreal forests: Data constrained design of a prognostic model of burned area for use in dynamic global vegetation models, *J. Geophys. Res.*, 112, D24112, doi:10.1029/2006JD008372.
Duncan, B. N., J. A. Logan, I. Bey, I. A. Megretskaia, R. M. Yantosca, P. C. Novelli, N. B. Jones, and C. P. Rinsland (2007), Global budget of CO, 1988–1997: Source estimates and validation with a global model, *J. Geophys. Res.*, 112, D22301, doi:10.1029/2007JD008459.
Eckhardt, S., A. Stohl, S. Beirle, N. Spichtinger, P. James, C. Forster, C. Junker, T. Wagner, U. Platt, and S. G. Jennings (2003), The North Atlantic Oscillation controls air pollution transport to the Arctic, *Atmos. Chem. Phys.*, 3, 1769–1778.
Fauria, M. M., and E. A. Johnson (2008), Climate and wildfires in the North American boreal forest, *Philos. Trans. R. Soc. B*, 363, 2317–2329. doi:10.1098/rstb.2007.2202.
Fisher, J. A., et al. (2010), Source attribution and interannual variability of Arctic pollution in spring constrained by aircraft (ARCTAS, ARCPAC) and satellite (AIRS) observations of carbon monoxide, *Atmos. Chem. Phys.*, 10, 977–996.
Flannigan, M. D., M. A. Krawchuk, W. J. de Groot, B. M. Wotton, and L. M. Gowman (2009) Implications of changing climate for global wildland fire, *Int. J. Wildland Fire*, 18, 483–507.
Kitzberger, T., P. M. Brown, E. K. Heyerdahl, T. W. Swetnam, and T. T. Veblen (2007), Contingent Pacific–Atlantic Ocean influence on multicentury wildfire synchrony over western North America, *Proc. Natl. Acad. Sci. U. S. A.*, 104, 343–548.
Lamarque, J.-F., et al. (2010), Historical (1850–2000) gridded anthropogenic and biomass burning emissions of reactive trace gases and aerosols: Methodology and application, *Atmos. Chem. Phys.*, 10, 7017–7039.
Le Goff, H., M. D. Flannigan, Y. Bergeron, and M. P. Girardin (2007) Historical fire regime shifts related to climate teleconnections in the Waswanipi area, central Quebec, Canada, *Int. J. Wildland Fire*, 16, 607–618.
Legrand, M., M. De Angelis, T. Staffelbach, A. Neftel, and B. Stauffer (1992), Large perturbations of ammonium and organic acids content in the summit Greenland Ice Core: Fingerprint from forest fires?, *Geophys. Res. Lett.*, 19, 473–475, doi:10.1029/91GL03121.
Liu, Y., J. Stanturf, and S. Goodrick (2010), Trends in global wildfire potential in a changing climate, *For. Ecol. Manage.*, 259, 685–697.
Novelli, P. C., K. A. Masarie, and P. M. Lang (1998), Distributions and recent changes of carbon monoxide in the lower troposphere, *J. Geophys. Res.*, 103, 19,015–19,033, doi:10.1029/98JD01366.
Olivier, J., J. Peters, C. Granier, G. Petron, J. Müller, and S. Wallens (2003), Present and future surface emissions of atmospheric compounds, *POET Rep. 2, EU Proj. EVK2-1999-00011*, ACCENT, Paris. [Available at http://www.aero.jussieu.fr/projet/ACCENT/POET.php.]
Patra, P. K., et al. (2011), TransCom model simulations of CH_4 and related species: Linking transport, surface flux and chemical loss with CH_4 variability in the troposphere and lower stratosphere, *Atmos. Chem. Phys.*, 11, 12,813–12,837.
Rahn, K. A. (1985), Progress in Arctic air chemistry, 1980–1984, *Atmos. Environ.*, 19, 1987–1994.
Randerson, J. T., et al. (2006), The impact of boreal forest fire on climate warming, *Science*, 314(5802), 1130–1132.
Ropelewski, C. F., and M. S. Halpert, (1986), North-American precipitation and temperature patterns associated with the El Niño–Southern Oscillation (ENSO), *Mon. Weather Rev.*, 114, 2352–2362.
Shindell, D. (2007), Local and remote contributions to Arctic warming, *Geophys. Res. Lett.*, 34, L14704, doi:10.1029/2007GL030221.
Shindell, D. T., et al. (2008), A multi-model assessment of pollution transport to the Arctic, *Atmos. Chem. Phys.*, 8, 5353–5372.
Skinner, W. R., A. Shabbar, M. D. Flannigan, and K. Logan (2006), Large forest fires in Canada and the relationship to global sea surface temperatures, *J. Geophys. Res.*, 111, D14106, doi:10.1029/2005JD006738.
Sodemann, H., et al. (2011) Episodes of cross-polar transport in the Arctic troposphere during July 2008 as seen from models, satellite, and aircraft observations, *Atmos. Chem. Phys.*, 11, 3631–3651.

Stohl, A., et al. (2007), Arctic smoke- record high air pollution levels in the European Arctic due to agricultural fires in eastern Europe in spring 2006, *Atmos. Chem. Phys.*, *7*, 511–534.

Szopa, S., D. A. Hauglustaine, and P. Ciais (2007), Relative contributions of biomass burning emissions and atmospheric transport to carbon monoxide interannual variability, *Geophys. Res. Lett.*, *34*, L18810, doi:10.1029/2007GL030231.

Trenberth, K. E. (1997), The definition of El Niño, *Bull. Am. Meteorol. Soc.*, *78*, 2771–2777.

van de Werf, G. R., J. T. Randerson, L. Giglio, G. J. Collatz, P. S. Kasibhatla, and A. F. Arellano (2006), Interannual variability in global biomass burning emissions from 1997 to 2004, *Atmos. Chem. Phys.*, *6*, 3423–3441.

van de Werf, G. R., J. T. Randerson, L. Giglio, G. J. Collatz, M. Mu, P. S. Kasibhatla, D. C. Morton, R. S. DeFries, Y. Jin, and T. T. van Leeuwen (2010), Global fire emissions and the contribution of deforestation, savanna, forest, agricultural, and peat fires (1997–2009), *Atmos. Chem. Phys.*, *10*, 11707–11735.

Westerling, A. L., H. G. Hidalgo, D. R. Cayan, and T. W. Swetnam (2006), Warming and earlier spring increase western U.S. forest wildfire activity, *Science*, *313*, 940–943.

Wofsy, S. C., et al. (1992), Atmospheric chemistry in the Arctic and subarctic: Influence of natural fires, industrial emissions, and stratospheric input, *J. Geophys. Res.*, *97*, 16,731–16,746, doi:10.1029/92JD00622.